mathematics

MDPI

Article

Epidemiological Investigation: Important Measures for the Prevention and Control of COVID-19 Epidemic in China

Cheng-Cheng Zhu [1], Jiang Zhu [2,*] and Jie Shao [3]

[1] School of Science, Jiangnan University, Wuxi 214122, China; chengchengzhu@jiangnan.edu.cn
[2] School of Mathematics and Statistics, Jiangsu Normal University, Xuzhou 221116, China
[3] School of Business, University of Science and Technology of China, Hefei 230026, China; jieshao@mail.ustc.edu.cn
* Correspondence: jiangzhu@jsnu.edu.cn

Abstract: Based on China's summary of three years of experience and measures in the prevention and control of the COVID-19 epidemic, we have built a COVID-19 prevention and control model integrating health and medical detection, big data information technology to track the trend of the epidemic throughout the whole process, isolation of key epidemic areas, and dynamic prevention and control management throughout the whole process. This model provides a simple, feasible, and theoretically reliable prevention and control model for future large-scale infectious disease prevention and control. The Lyapnov functional method is replaced by the global exponential attractor theory, which provides a new mathematical method for studying the global stability of the multi parameter, multi variable infectious disease prevention and control system. We extracted mathematical methods and models suitable for non-mathematical infectious disease researchers from profound and difficult to understand mathematical theories. Using the results of the global exponential Attractor theory obtained in this paper, we studied the global dynamics of the COVID-19 model with an epidemiological investigation. The results demonstrated that the non-constant disease-free equilibrium is globally asymptotically stable when $\lambda^* < 0$, and the COVID-19 epidemic is persisting uniformly when $\lambda^* > 0$. In order to understand the impact of the epidemiological investigation under different prevention and control stages in China, we compare the control effects of COVID-19 under different levels of epidemiological investigation policies. We visually demonstrate the global stability and global exponential attractiveness of the COVID-19 model with transferors between regions and epidemiological investigation in a temporal-spatial heterogeneous environment with the help of numerical simulations. We find that the epidemiological investigation really has a significant effect on the prevention and control of the epidemic situation, and we can also intuitively observe the relationship between the flow of people (including tourism, shopping, work and so on) and epidemiological investigation policies. Our model is adapted to different stages of prevention and control; the emergency "circuit breaker" mechanism of the model is also consistent with actual prevention and control.

Keywords: global exponentially attracting set; temporal-spatial heterogeneous COVID-19 model; epidemiological investigation

MSC: 35B41; 35K57; 35B35; 37N25; 92D25; 92D30

Citation: Zhu, C.-C.; Zhu, J.; Shao, J. Epidemiological Investigation: Important Measures for the Prevention and Control of COVID-19 Epidemic in China. *Mathematics* **2023**, *11*, 3027. https://doi.org/10.3390/math11133027

Academic Editor: Takashi Suzuki

Received: 4 June 2023
Revised: 4 July 2023
Accepted: 6 July 2023
Published: 7 July 2023

1. Introduction

The epidemic of novel coronavirus pneumonia has spread around the world for three years [1–5]. As a self-limiting epidemic in a temporal-spatial heterogeneous environment [6], different countries have formulated different prevention and control policies according to their national conditions. For the prevention and control of the COVID-19 epidemic, governments and medical staff have made great efforts in the past three years.

Researchers have also expressed their opinions and proposed many different control methods and prevention strategies. The prevention and control of COVID-19 is different for different countries and regions [7–12]. Akter and Jin [13] propose a Caputo-based fractional compartmental model for the dynamics of the novel COVID-19. Martinez-Fernandez et al. [14] compared Verhulst's, Gompertz's, and SIR models from the point of view of their efficiency to describe the behavior of COVID-19 in Spain. These mathematical models are used to predict the future of the pandemic by first solving the corresponding inverse problems to identify the model parameters in each wave separately, using the observed data in daily cases in the past [15]. In the beginning of the COVID-19 pandemic, universities have experienced unique challenges due to their dual nature as a place of education and residence. Up to now, China has been a country with a very low fatality ratio of COVID-19. The lowest fatality ratio of COVID-19 in the world is due to the strict epidemiological investigation policy of the Chinese government. These epidemiological investigation policies include big data screening, travel reports and national nucleic acid testing. At the beginning of December 2022, the Chinese government made timely adjustments to relax the prevention and control strategy in response to the domestic epidemic spread trend, and canceled the nationwide nucleic acid, travel reports and other epidemiological investigations. The current epidemiological investigation strategy has changed into finding out the base number and situation of key populations, and strengthening health monitoring and early intervention. After the relaxation of epidemiological investigations, there has been a rapid and significant increase in the number of infected people in China. China's epidemiological investigation policy has its own characteristics in global epidemic prevention and control policies. According to data released by the WHO under this type of prevention and control, only 33,144 people in China have died from COVID-19. We believe that the prevention and control strategy of this epidemiological investigation can serve as an experience to learn from, and we can also try this strategy in future outbreaks similar to COVID-19.

The purpose of this article is to study the positive impact of epidemiological investigations on epidemic prevention and control through mathematical modeling methods.

In order to use mathematical theory to analyze the rationality and effectiveness of epidemiological investigation under different prevention and control stages in China, we construct a COVID-19 model with transferors between regions, an epidemiological investigation and a relapse in a temporal-spatial heterogeneous environment. Our model is divided into six compartments, namely susceptible individuals (S), latent patients (L), transferors between regions (T), infected individuals (I), persons under epidemiological investigation (E), temporary restorers (R) and healthy individuals (H). The parameters description and transfer diagram as shown in Table 1 and Figure 1.

Table 1. State variables and parameters of COVID-19 ($SLTEIRH$) model.

Parameter	Description
$\Lambda(x,t)$	Total recruitment scale into this homogeneous social mixing community at location x and time t.
$\beta_i(x,t), i=1,2$	Contact rate at location x and time t.
$\alpha(x,t), \sigma(x,t), \nu_2(x,t)$	Infection rate at location x and time t.
$\delta(x,t)$	Contact rate when moving between regions at location x and time t.
$\gamma(x,t)$	Rate of epidemiological investigation at location x and time t.
$\theta_1(x,t)$	Release rate of epidemiological investigation at location x and time t.
$\theta_2(x,t)$	Complete cure rate at location x and time t.
$\rho(x,t)$	Relapse rate at location x and time t.
$\phi(x,t)$	Per-capita recovery (treatment) rate at location x and time t.
$\omega(x,t)$	Interregional transfer rate of patients with incubation period and asymptomatic infection at location x and time t.
$\nu_1(x,t)$	Asymptomatic infection rate at location x and time t.
$\mu(x,t)$	Natural mortality rate at location x and time t.
$\eta_i(x,t), i=1,2,3$	Fatality ratio at location x and time t.
k	Epidemiological investigation proportions at different stages of prevention and control.

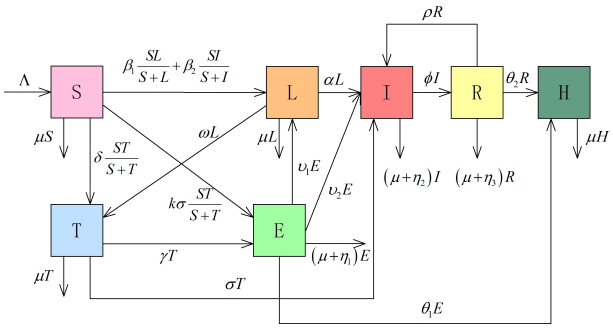

Figure 1. Transfer diagram for the COVID-19 ($SLTEIRH$) model with transferors between regions, epidemiological investigation and relapse in a temporal-spatial heterogeneous environment.

From Figure 1, the following system with the initial-boundary-value conditions is constructed by:

$$
\begin{cases}
\frac{\partial S}{\partial t} = \nabla\cdot(d_S(x)\nabla S) + \Lambda(x,t) - \beta_1(x,t)\frac{SL}{S+L} - \beta_2(x,t)\frac{SI}{S+I} \\
\quad - \delta(x,t)\frac{ST}{S+T} - k\sigma(x,t)\frac{ST}{S+T} - \mu(x,t)S, \\
\frac{\partial L}{\partial t} = \nabla\cdot(d_L(x)\nabla L) + \beta_1(x,t)\frac{SL}{S+L} + \beta_2(x,t)\frac{SI}{S+I} + \nu_1(x,t)E \\
\quad - [\mu(x,t) + \omega(x,t) + \alpha(x,t)]L, \\
\frac{\partial T}{\partial t} = \nabla\cdot(d_T(x)\nabla T) + \delta(x,t)\frac{ST}{S+T} + \omega(x,t)L \\
\quad - [\mu(x,t) + \gamma(x,t) + \sigma(x,t)]T, \\
\frac{\partial E}{\partial t} = \gamma(x,t)T + k\sigma(x,t)\frac{ST}{S+T} \\
\quad - [\mu(x,t) + \eta_1(x,t) + \nu_1(x,t) + \nu_2(x,t) + \theta_1(x,t)]E, \\
\frac{\partial I}{\partial t} = \nabla\cdot(d_I(x)\nabla I) + \alpha(x,t)L + \sigma(x,t)T + \nu_2(x,t)E + \rho(x,t)R \\
\quad - [\mu(x,t) + \eta_2(x,t) + \phi(x,t)]I, \\
\frac{\partial R}{\partial t} = \nabla\cdot(d_R(x)\nabla R) + \phi(x,t)I - [\mu(x,t) + \eta_3(x,t) + \rho(x,t) + \theta_2(x,t)]R, \\
\frac{\partial H}{\partial t} = \nabla\cdot(d_H(x)\nabla H) + \theta_1(x,t)E + \theta_2(x,t)R - \mu(x,t)H, \\
\quad x\in\Omega, t>0, \\
\frac{\partial S}{\partial \mathbf{n}} = \frac{\partial L}{\partial \mathbf{n}} = \frac{\partial T}{\partial \mathbf{n}} = \frac{\partial E}{\partial \mathbf{n}} = \frac{\partial I}{\partial \mathbf{n}} = \frac{\partial R}{\partial \mathbf{n}} = \frac{\partial H}{\partial \mathbf{n}} = 0,\ x\in\partial\Omega, t>0, \\
S(x,0) = S_0(x) \geq 0, L(x,0) = L_0(x) \geq 0, T(x,0) = T_0(x) \geq 0, \\
E(x,0) = E_0(x) \geq 0, I(x,0) = I_0(x) \geq 0, R(x,0) = R_0(x) \geq 0, \\
H(x,0) = H_0(x) \geq 0, x\in\Omega.
\end{cases}
\tag{1}
$$

Here, Ω is a bounded domain in $\mathbb{R}^m (m \geq 1)$ with smooth boundary $\partial\Omega$ (when $m > 1$), $d_S(x), d_L(x), d_T(x), d_I(x), d_R(x), d_H(x) \in \mathbf{C}^1(\Omega)$ are positive, continuous and uniformly bounded diffusion coefficients depending on space.Since most of the people who participated in the epidemiological investigation were quarantined at home or in the hospital, we do not consider the diffusion of them in this article. $\Lambda(x,t), \beta_1(x,t), \beta_2(x,t), \rho(x,t), \nu_1(x,t), \nu_2(x,t), \alpha(x,t), \omega(x,t), \delta(x,t), \sigma(x,t), \theta_1(x,t), \theta_2(x,t), \gamma(x,t), \phi(x,t), \mu(x,t), \eta_1(x,t), \eta_2(x,t)$ and $\eta_3(x,t)$ are bounded and positive Hölder continuous functions on accounting; k represents the proportion of epidemiological investigation of susceptible persons. Neumann boundary conditions $\frac{\partial S}{\partial \mathbf{n}} = \frac{\partial L}{\partial \mathbf{n}} = \frac{\partial T}{\partial \mathbf{n}} = \frac{\partial E}{\partial \mathbf{n}} = \frac{\partial I}{\partial \mathbf{n}} = \frac{\partial R}{\partial \mathbf{n}} = \frac{\partial H}{\partial \mathbf{n}} = 0$ denotes that the change rate on the boundary of the region Ω is equal to 0. It is straightforward to verify that $\frac{SI}{S+I}\left(\frac{SL}{S+L}, \frac{ST}{S+T}\right)$ is a Lipschitz continuous function of S and $I(L,T)$ in the open first quadrant. Therefore, we can extend it to the entire first quadrant by defining it to be zero whenever $S = 0$ or $I = 0$ $(L = 0, T = 0)$. Throughout the paper, we assume that the initial value S_0, L_0, T_0, E_0, I_0 and R_0 are nonnegative continuous functions on $\overline{\Omega}$, and the number of infected individuals is positive, i.e., $\int_\Omega I_0(x)dx > 0$. Specific parameters described in Table 1.

The highlight of this model is to examine the impact of epidemiological investigation on epidemic prevention and control. Epidemiological investigation policies at different stages can be adjusted through the parameter k in the model to achieve the best prevention and control effect. The epidemiological investigation in the model can be understood as a comprehensive compartment including the nucleic acid test, big data monitoring, and even vaccination. Of course, we can also refine compartment E in the process of modeling. However, in addition to increasing the difficulty of mathematical reasoning, this refinement will not have a significant impact on the long-term dynamic behavior of the model. Therefore, it is appropriate for us to select a comprehensive compartment for this epidemic investigation. Taking the spread of the COVID-19 epidemic as the research object, combined with the current development of the COVID-19 epidemic, Yang et al. [16] sorts out the relevant mathematical models for the study of the spread of COVID-19, among which the models based on the SIR model and SEIR model and the mathematical models combined with these two models are mainly selected. Finally, the importance of the reasonable and effective control of parameters and multi-model combined modeling is pointed out forthe future.

The organization of this paper is as follows. In Section 2, we first provide a sufficient condition for the existence of the global exponentially attracting set, which can be more easily applied to specific models. Second, we prove the existence of the system (1), and then we obtain the global stability and persistence of the COVID-19 epidemic with an epidemiological investigation. In Section 3, we simulate the impact of the epidemiological investigation and travel on the prevention and control of COVID-19 in China. By adjusting the proportion of the epidemiological investigation, we simulate the spread of the COVID-19 epidemic under different epidemiological investigations. In Section 4, we provide our conclusions and some discussions.

2. The Effectiveness Analysis of Epidemiological Investigation

Because the structure of the epidemiological investigation model (1) is complex, it contains multiple coupled state variables, and the coefficients are all temporal-spatial heterogeneous except for the spatially heterogeneous diffusion coefficient. It is tedious and difficult to discuss the global stability of system (1) by adopting the usual method of constructing Lyapunov functionals. For these reasons, we need to seek new breakthroughs in methods and find some new methods and means to solve the stability analysis problems of systems with a large number of equations. It is well known that the global attractor theory can discuss the dynamics of dissipative evolutionary systems. However, the existing global attractor and even global exponential attractor theories are all abstract conditions that are esoteric and difficult to understand in mathematical theory. They are difficult to apply directly to actual mathematical models. This seriously hinders the general infectious disease researchers from applying these mathematical theories to understand and discover the laws of disease transmission. Through our previous studies [6,17], we have tried many times to discuss the transmission of some specific diseases with the help of the global attractor theory in infinite-dimensional dynamical systems and have achieved good results. Therefore, we hope to continue these efforts and obtain some more convenient conditions that can be applied directly.

Let $\mathbf{H}$ be Hilbert space; $\mathbf{H}_1 \subset \mathbf{H}$ is a dense and compact inclusion. $A : \mathbf{H}_1 \to \mathbf{H}$ is a symmetrical sectorial operator and all eigenvalues of A are

$$0 > \lambda_1 \geq \lambda_2 \geq \cdots \geq \lambda_k > \ldots, \ \lambda_k \to -\infty \ (k \to \infty), \tag{2}$$

Consider the system of reaction diffusion equations

$$\begin{cases} \frac{du}{dt} = Au + G(t,u), \\ u(0) = u_0. \end{cases} \tag{3}$$

In the following lemma, we provide a sufficient condition to prove the global exponentially attracting set of system (3). This condition is more convenient in terms of computation and workload compared with our previous research results in the verification process of the actual model.

Theorem 1. *Assume that condition (2) holds, and there exists a constant $C > 0$ such that for any bounded set $\mathbf{B}$, there exists a constant $t_{\mathbf{B}} > 0$, such that for $\forall u_0 \in \mathbf{B} \subset \mathbf{H}_1$, the solution $u = u(t, u_0)$ of system (3) satisfies condition*

$$\langle G(t,u), u\rangle_{\mathbf{H}} \leq C, \forall t \geq t_{\mathbf{B}}, \tag{4}$$

then, in the system (3) exists a global exponentially attracting set $\widetilde{\mathcal{A}^*}$; it exponentially attracts any bounded set under the $\mathbf{H}$-norm.

Proof. Assume that $u = u(t, u_0)$ is a solution of the system (3), where $u_0 \in \mathbf{B}$. Then, by the definition of the fractional power subspace generated by sectorial operator A, we can obtain that

$$\begin{aligned} \langle Au + G(t,u), u\rangle_{\mathbf{H}} &= \langle Au, u\rangle_{\mathbf{H}} + \langle G(t,u), u\rangle_{\mathbf{H}} \\ &= -\|u\|^2_{\mathbf{H}_{\frac{1}{2}}} + \langle G(t,u), u\rangle_{\mathbf{H}} \\ &\leq -\|u\|^2_{\mathbf{H}_{\frac{1}{2}}} + C, \forall t \geq t_{\mathbf{B}}. \end{aligned} \tag{5}$$

Since A: $\mathbf{H}_1 \to \mathbf{H}$ is a symmetrical sectorial operator, the eigenvectors $\{e_j\}_{j\in\mathbb{N}}$ corresponding to the eigenvalues $\{\lambda_j\}_{j\in\mathbb{N}}$ are a complete orthonormal base of $\mathbf{H}$. For any $u \in \mathbf{H}$, assume that u can be presented as

$$u = \sum_{i=1}^{\infty} x_i e_i, \|u\|^2_{\mathbf{H}} = \sum_{i=1}^{\infty} x_i^2.$$

In addition, it follows from $\lim\limits_{j\to\infty} \lambda_j = -\infty$ that for any $N > 0$, there is an integral number $J \geq 1$, such that $-N \geq \lambda_j, \forall j \geq J+1$.

Let

$$\mathbf{H}_1^J = span\{e_1, e_2, \ldots, e_J\} \text{ and } \mathbf{H}_2^J = \left(\mathbf{H}_1^J\right)^{\perp}.$$

Then, each $u \in \mathbf{H}$ can be decomposed as

$$\begin{aligned} u &= Pu + (I-P)u := u_1 + u_2, \\ u_1 &= \sum_{i=1}^{J} x_i e_i \in \mathbf{H}_1^J,\ u_2 = \sum_{i=J+1}^{\infty} x_i e_i \in \mathbf{H}_2^J, \end{aligned}$$

where P: $\mathbf{H} \to \mathbf{H}_1^J$ is the projector.

By using the condition (5), there exists positive constants $C > 0$, such that for any bounded set $\mathbf{B} \subset \mathbf{H}_1$, there exists a $t_{\mathbf{B}} > 0$, which satisfies that

$$\frac{1}{2}\frac{d}{dt}\langle u, u\rangle_{\mathbf{H}} = \left\langle \dot{u}, u\right\rangle_{\mathbf{H}} = \langle Au + G(t,u), u\rangle_{\mathbf{H}} \leq -\|u\|^2_{\mathbf{H}_{\frac{1}{2}}} + C.$$

Since $\mathbf{H}_{\frac{1}{2}} \hookrightarrow \mathbf{H}$, there exists $C_1 > 0$, such that

$$\|u\|_{\mathbf{H}_{\frac{1}{2}}} \geq C_1 \|u\|_{\mathbf{H}}, \ \forall u \in \mathbf{H}_{\frac{1}{2}}.$$

Hence,

$$\frac{1}{2}\frac{d}{dt}\|u\|_{\mathbf{H}}^2 \leq -C_1^2\|u\|_{\mathbf{H}}^2 + C,$$

By Gronwall's inequality in differential form Lemma 2.3 of [18], we obtain that

$$\|u\|_{\mathbf{H}}^2 \leq e^{-\alpha t}\|u_0\|_{\mathbf{H}}^2 + \frac{2C}{\alpha}(1 - e^{-\alpha t}), \tag{6}$$

where $\alpha = 2C_1^2$. Assume that $r > 0$, such that $\frac{2C}{\alpha} < r^2$. Since B is bounded, there exists a constant $K_B > 0$, such that for any $u_0 \in B, \|u_0\|_{\mathbf{H}} \leq K_B$. It follows from (6) that if we take t_B big enough, such that $\|u(t,u_0)\|_{\mathbf{H}}^2 = \|\mathcal{Q}(t)u_0\|_{\mathbf{H}}^2 \leq r^2, \forall t \geq t_B$. Hence, $B_r \subset H$ is an absorbing set. Moreover, this implies that

$$\|P\mathcal{Q}(t)u_0\|_{\mathbf{H}} \leq r, \ \forall t \geq t_B.$$

It means that $\{\|P\mathcal{Q}(t)\mathbf{B}\|_{\mathbf{H}}\}_{t\geq t_{\mathbf{B}}}$ is bounded.
It follows that from the inner product of Equation (3) in $\mathbf{H}$ with u_2, we have

$$\begin{aligned}
\frac{1}{2}\frac{d}{dt}\langle u, u_2\rangle_{\mathbf{H}} &= \frac{1}{2}\frac{d}{dt}\langle u_2, u_2\rangle_{\mathbf{H}} = \frac{1}{2}\frac{d}{dt}\langle u, u - u_1\rangle_{\mathbf{H}} \\
&= \frac{1}{2}\frac{d}{dt}\langle u, u\rangle_{\mathbf{H}} - \frac{1}{2}\frac{d}{dt}\langle u_1, u_1\rangle_{\mathbf{H}} \\
&= \left\langle \dot{u}, u\right\rangle_{\mathbf{H}} - \left\langle \dot{u}_1, u_1\right\rangle_{\mathbf{H}} \\
&= \langle Au + G(t,u), u\rangle_{\mathbf{H}} - \left\langle \dot{u}_1, u_1\right\rangle_{\mathbf{H}} \\
&\leq -\|u\|_{\mathbf{H}_{\frac{1}{2}}}^2 + C - \left\langle \dot{u}_1, u_1\right\rangle_{\mathbf{H}}, \forall t \geq t_{\mathbf{B}},
\end{aligned} \tag{7}$$

and

$$\begin{aligned}
\langle Au_2, u_2\rangle_{\mathbf{H}} &= -\|u_2\|_{\mathbf{H}_{\frac{1}{2}}}^2 \\
&= \sum_{i=J+1}^{\infty} \lambda_i x_i^2 \\
&\leq -N\sum_{i=J+1}^{\infty} x_i^2 = -N\|u_2\|_{\mathbf{H}}^2.
\end{aligned} \tag{8}$$

Note that

$$\begin{aligned}
\langle Au, u\rangle_{\mathbf{H}} &= \langle A(u_1+u_2), u_1+u_2\rangle_{\mathbf{H}} \\
&= \langle Au_1, u_1\rangle_{\mathbf{H}} + \langle Au_2, u_2\rangle_{\mathbf{H}} \\
&= -\|u_1\|_{\mathbf{H}_{\frac{1}{2}}}^2 - \|u_2\|_{\mathbf{H}_{\frac{1}{2}}}^2,
\end{aligned}$$

it follows from (7) and (8) that

$$\begin{aligned}
\frac{1}{2}\frac{d}{dt}\langle u_2, u_2\rangle_{\mathbf{H}} &\leq -\|u\|_{\mathbf{H}_{\frac{1}{2}}}^2 + C - \frac{1}{2}\frac{d}{dt}\langle u_1, u_1\rangle_{\mathbf{H}} \\
&\leq -N\|u_2\|_{\mathbf{H}}^2 + C - \frac{1}{2}\frac{d}{dt}\langle u_1, u_1\rangle_{\mathbf{H}}, \forall t \geq t_{\mathbf{B}}.
\end{aligned}$$

By integrating both ends of this inequality, we can obtain that

$$\|u_2\|_{\mathbf{H}}^2 \leq -2N\int_{t_B}^{t}\|u_2\|_{\mathbf{H}}^2 ds + 2C(t - t_B) + \|u(t_B)\|_{\mathbf{H}}^2$$

$$\leq \quad -2N\int_{t_B}^{t}\|u_2\|_{\mathbf{H}}^2 ds + 2C(t-t_B) + r^2.$$

By Gronwall's inequality, we have that

$$\|u_2\|_{\mathbf{H}}^2 \leq e^{-2N(t-t_{\mathbf{B}})}r^2 + \frac{C}{N}\left(1 - e^{-2N(t-t_{\mathbf{B}})}\right), \forall t \geq t_{\mathbf{B}}$$

and $N > 0$ is arbitrary. Therefore, N is large enough, such that $\frac{C}{N} < \varepsilon$; then, we deduce that the **Condition (C*)** of [19] holds. Hence, it follows from Theorems 3.3 and 4.1 in [19] that in the system (3) exists a global exponentially attracting set $\widehat{\mathcal{A}^*}$; it exponentially attracts any bounded set under the **H**-norm. □

From now on, we denote that $\mathbf{H} = \mathbf{L}^2(\Omega)$, $\mathbf{H}_1 = \mathbf{H}_0^1(\Omega) \cap \mathbf{C}^{2,1}(\Omega)$, $\mathbf{H}^7 = \mathbf{H} \times \mathbf{H} \times \mathbf{H} \times \mathbf{H} \times \mathbf{H} \times \mathbf{H} \times \mathbf{H}$ and $\mathbf{H}_1^7 = \mathbf{H}_1 \times \mathbf{H}_1 \times \mathbf{H}_1 \times \mathbf{H}_1 \times \mathbf{H}_1 \times \mathbf{H}_1 \times \mathbf{H}_1$. Note that $\mathbf{H}^7$ and $\mathbf{H}_1^7$ are Banach spaces equipped with norm

$$\left\|(S, L, T, E, I, R)^T\right\|_{\mathbf{H}^7} := \max\{\|S\|_{\mathbf{H}}, \|L\|_{\mathbf{H}}, \|T\|_{\mathbf{H}}, \|E\|_{\mathbf{H}}, \|I\|_{\mathbf{H}}, \|R\|_{\mathbf{H}}, \|H\|_{\mathbf{H}}\} \tag{9}$$

and

$$\left\|(S, L, T, E, I, R)^T\right\|_{\mathbf{H}_1^7} := \max\left\{\|S\|_{\mathbf{H}_1}, \|L\|_{\mathbf{H}_1}, \|T\|_{\mathbf{H}_1}, \|E\|_{\mathbf{H}_1}, \|I\|_{\mathbf{H}_1}, \|R\|_{\mathbf{H}_1}, \|H\|_{\mathbf{H}_1}\right\}.$$

For any given continuous function f on $\overline{\Omega} \times (0, +\infty)$, we denote

$$\begin{aligned} f^*(t) &= \sup_{x\in\overline{\Omega}} f(x,t) \text{ and } f_*(t) = \inf_{x\in\overline{\Omega}} f(x,t), \\ f^* &= \sup_{x\in\overline{\Omega}, t>0} f(x,t) \text{ and } f_* = \inf_{x\in\overline{\Omega}, t>0} f(x,t). \end{aligned}$$

By the similar method used in [17], we can prove the following existence, positivity and boundedness of the global solution of the system (1).

Theorem 2. *For each* $(S_0(x), L_0(x), T_0(x), E_0(x), I_0(x), R_0(x), H(x)) \in \mathbf{C}(\overline{\Omega} \times [-\tau, 0])$, *system (1) exists a positive and uniformly bounded global solution* $(S(x,t), L(x,t), T(x,t), E(x,t), I(x,t), R(x,t), H(x,t)) \in \mathbf{C}^{2,1}(\Omega \times (-\tau, \infty))$.

Proof. Since

$$\begin{aligned} A &= (\nabla \cdot (d_S(x)\nabla), \nabla \cdot (d_L(x)\nabla), \nabla \cdot (d_T(x)\nabla), 0, \\ &\quad \nabla \cdot (d_I(x)\nabla), \nabla \cdot (d_R(x)\nabla), \nabla \cdot (d_H(x)\nabla)) \end{aligned}$$

is a symmetrical sectorial operator and all eigenvalues of L are

$$0 > \lambda_1 \geq \lambda_2 \geq \cdots \geq \lambda_K > \ldots, \ \lambda_K \to -\infty \ (K \to \infty),$$

Let

$$\begin{aligned} &G(S, L, T, E, I, R, H) := (g_1(S, L, T, E, I, R, H), g_2(S, L, T, E, I, R, H), \\ &g_3(S, L, T, E, I, R, H), g_4(S, L, T, E, I, R, H), g_5(S, L, T, E, I, R, H) \\ &g_6(S, L, T, E, I, R, H), g_7(S, L, T, E, I, R, H))^T, \end{aligned}$$

where

$$\begin{aligned} g_1(S, L, T, E, I, R, H) &= \Lambda(x,t) - \beta_1(x,t)\frac{SL}{S+L} - \beta_2(x,t)\frac{SI}{S+I} \\ &\quad -\delta(x,t)\frac{ST}{S+T} - k\sigma(x,t)\frac{ST}{S+T} - \mu(x,t)S, \end{aligned}$$

$$
\begin{aligned}
g_2(S,L,T,E,I,R,H) &= \beta_1(x,t)\frac{SL}{S+L}+\beta_2(x,t)\frac{SI}{S+I}+\nu_1(x,t)E\\
&\quad -[\mu(x,t)+\omega(x,t)+\alpha(x,t)]L,\\
g_3(S,L,T,E,I,R,H) &= \delta(x,t)\frac{ST}{S+T}+\omega(x,t)L-[\mu(x,t)+\gamma(x,t)+\sigma(x,t)]T,\\
g_4(S,L,T,E,I,R,H) &= \gamma(x,t)T+k\sigma(x,t)\frac{ST}{S+T}\\
&\quad -[\mu(x,t)+\eta_1(x,t)+\nu_1(x,t)+\nu_2(x,t)+\theta_1(x,t)]E,\\
g_5(S,L,T,E,I,R,H) &= \alpha(x,t)L+\sigma(x,t)T+\nu_2(x,t)E+\rho(x,t)R\\
&\quad -[\mu(x,t)+\eta_2(x,t)+\phi(x,t)]I,\\
g_6(S,L,T,E,I,R,H) &= \phi(x,t)I-[\mu(x,t)+\eta_3(x,t)+\rho(x,t)+\theta_2(x,t)]R,\\
g_7(S,L,T,E,I,R,H) &= \theta_1(x,t)E+\theta_2(x,t)R-\mu(x,t)H
\end{aligned}
$$

In addition, by means of the differential mean value theorem of multivariate functions and (9),

$$
\begin{aligned}
&\|g_1(S_1,L_1,T_1,E_1,I_1,R_1,H_1)-g_1(S_2,L_2,T_2,E_2,I_2,R_2,H_2)\|_{\mathbf{H}}\\
=\;&\Big\|-\beta_1(x,t)\Big(\tfrac{S_1L_1}{S_1+L_1}-\tfrac{S_2L_2}{S_2+L_2}\Big)-\beta_2(x,t)\Big(\tfrac{S_1I_1}{S_1+I_1}-\tfrac{S_2I_2}{S_2+I_2}\Big)\\
&-[\delta(x,t)+k\sigma(x,t)]\Big(\tfrac{S_1T_1}{S_1+T_1}-\tfrac{S_2T_2}{S_2+T_2}\Big)-\mu(x,t)(S_1-S_2)\Big\|_{\mathbf{H}}\\
\le\;&\beta_1^*(t)\|u-v\|_{\mathbf{H}}+\beta_2^*(t)\|u-v\|_{\mathbf{H}}+(\delta^*(t)+k\sigma^*(t))\|u-v\|_{\mathbf{H}}\\
&+\mu^*(t)\|u-v\|_{\mathbf{H}}\\
=\;&\big(\beta_1^*(t)+\beta_2^*(t)+\delta^*(t)+k\sigma^*(t)+\mu^*(t)\big)\|u-v\|_{\mathbf{H}},
\end{aligned}
$$

where $u=(S_1,L_1,T_1,E_1,I_1,R_1,H_1), v=(S_2,L_2,T_2,E_2,I_2,R_2,H_2)$. Similarly,

$$
\begin{aligned}
&\|g_2(S_1,L_1,T_1,E_1,I_1,R_1,H_1)-g_2(S_2,L_2,T_2,E_2,I_2,R_2,H_2)\|_{\mathbf{H}}\\
\le\;&\big(\beta_1^*(t)+\beta_2^*(t)+\nu_1^*(t)+\mu^*(t)+\alpha^*(t)+\omega^*(t)\big)\|u-v\|_{\mathbf{H}},
\end{aligned}
$$

$$
\begin{aligned}
&\|g_3(S_1,L_1,T_1,E_1,I_1,R_1,H_1)-g_3(S_2,L_2,T_2,E_2,I_2,R_2,H_2)\|_{\mathbf{H}}\\
\le\;&(\delta^*(t)+\omega^*(t)+\gamma^*(t)+\sigma^*(t)+\mu^*(t))\|u-v\|_{\mathbf{H}},
\end{aligned}
$$

$$
\begin{aligned}
&\|g_4(S_1,L_1,T_1,E_1,I_1,R_1,H_1)-g_4(S_2,L_2,T_2,E_2,I_2,R_2,H_2)\|_{\mathbf{H}}\\
\le\;&\big(\gamma^*(t)+k\sigma^*(t)\mu^*(t)+\eta_1^*(t)+\nu_1^*(t)+\nu_2^*(t)+\theta_1^*(t)\big)\|u-v\|_{\mathbf{H}},
\end{aligned}
$$

$$
\begin{aligned}
&\|g_5(S_1,L_1,T_1,E_1,I_1,R_1,H_1)-g_5(S_2,L_2,T_2,E_2,I_2,R_2,H_2)\|_{\mathbf{H}}\\
\le\;&(\alpha^*(t)+\sigma^*(t)+\nu_2^*(t)+\rho^*(t)+\mu^*(t)+\eta_2^*(t)+\phi^*(t))\|u-v\|_{\mathbf{H}},
\end{aligned}
$$

$$
\begin{aligned}
&\|g_6(S_1,L_1,T_1,E_1,I_1,R_1,H_1)-g_6(S_2,L_2,T_2,E_2,I_2,R_2,H_2)\|_{\mathbf{H}}\\
\le\;&(\phi^*(t)+\mu^*(t)+\eta_3^*(t)+\rho^*(t)+\theta_2^*(t))\|u-v\|_{\mathbf{H}},
\end{aligned}
$$

$$
\begin{aligned}
&\|g_7(S_1,L_1,T_1,E_1,I_1,R_1,H_1)-g_7(S_2,L_2,T_2,E_2,I_2,R_2,H_2)\|_{\mathbf{H}}\\
\le\;&\big(\theta_1^*(t)+\theta_2^*(t)+\mu^*(t)\big)\|u-v\|_{\mathbf{H}}.
\end{aligned}
$$

If we choose

$$
\begin{aligned}
h(t) = \max\{&\beta_1^*(t)+\beta_2^*(t)+\delta^*(t)+k\sigma^*(t)+\mu^*(t),\\
&\beta_1^*(t)+\beta_2^*(t)+\nu_1^*(t)+\mu^*(t)+\alpha^*(t)+\omega^*(t),\\
&\delta^*(t)+\omega^*(t)+\gamma^*(t)+\sigma^*(t)+\mu^*(t),\\
&\gamma^*(t)+k\sigma^*(t)\mu^*(t)+\eta_1^*(t)+\nu_1^*(t)+\nu_2^*(t)+\theta_1^*(t),\\
&\alpha^*(t)+\sigma^*(t)+\nu_2^*(t)+\rho^*(t)+\mu^*(t)+\eta_2^*(t)+\phi^*(t),\\
&\phi^*(t)+\mu^*(t)+\eta_3^*(t)+\rho^*(t)+\theta_2^*(t),\theta_1^*(t)+\theta_2^*(t)+\mu^*(t)\},
\end{aligned}
$$

then

$$\begin{aligned} & \|G(t,u)-G(t,v)\|_{\mathbf{H}^7} \\ = \; & \|(g_1(t,u)-g_1(t,v)),(g_2(t,u)-g_2(t,v)),(g_3(t,u)-g_3(t,v)), \\ & (g_4(t,u)-g_4(t,v)),(g_5(t,u)-g_5(t,v)), \\ & (g_6(t,u)-g_6(t,v)),(g_7(t,u)-g_7(t,v))\|_{\mathbf{H}^7} \\ = \; & \max\{\|g_1(t,u)-g_1(t,v)\|_{\mathbf{H}},\|g_2(t,u)-g_2(t,v)\|_{\mathbf{H}}, \\ & \|g_3(t,u)-g_3(t,v)\|_{\mathbf{H}},\|g_4(t,u)-g_4(t,v)\|_{\mathbf{H}},\|g_5(t,u)-g_5(t,v)\|_{\mathbf{H}}, \\ & \|g_6(t,u)-g_6(t,v)\|_{\mathbf{H}},\|g_7(t,u)-g_7(t,v)\|_{\mathbf{H}}\} \\ \leq \; & h(t)\cdot\|u-v\|_{\mathbf{H}^7}. \end{aligned}$$

Hence, the Lipschitz condition is well verified. Therefore, by Theorem 11.3.5 of [20] and Theorem 2.3 of [21], we can guarantee that in system (2) exists a global solution

$$(S(x,t),L(x,t),T(x,t),E(x,t),I(x,t),R(x,t),H(x,t))\in\mathbf{C}^{2,1}(\Omega\times(-\tau,\infty)).$$

According to the method in Lemma 2.1 and Theorem 2.2 of the recent paper [18], we can easily obtain the positivity of the global solution of the system (1). Moreover, by a similar proof of our recent Theorem 3.1 of [17], we can prove that the the global solution of the system (1) is bounded. □

Next, we prove the existence of the global exponentially attracting set of system (1) by verifying the condition (4). Then, we obtain the existence of the global exponentially attracting set of the system (1).

Theorem 3. *In system (1) exists a global exponentially attracting set $\mathcal{A}^*$; it exponentially attracts any bounded set in $\mathbf{H}^7$.*

Proof. We first verify condition (4).

$$\begin{aligned} & \left\langle \begin{array}{c} \Lambda(x,t)-\beta_1(x,t)\frac{SL}{S+L}-\beta_2(x,t)\frac{SI}{S+I} \\ -\delta(x,t)\frac{ST}{S+T}-k\sigma(x,t)\frac{ST}{S+T}-\mu(x,t)S \end{array}, \; S \right\rangle_{\mathbf{H}} \\ = & \int_\Omega \Lambda(x,t)Sdx-\int_\Omega \beta_1(x,t)\frac{S^2L}{S+L}dx-\int_\Omega \beta_2(x,t)\frac{S^2I}{S+I}dx \\ & -\int_\Omega[\delta(x,t)+k\sigma(x,t)]\frac{S^2T}{S+T}dx-\int_\Omega \mu(x,t)S^2dx \\ \leq & \Lambda^*\int_\Omega Sdx \end{aligned}$$

$$\begin{aligned} & \left\langle \begin{array}{c} \beta_1(x,t)\frac{SL}{S+L}+\beta_2(x,t)\frac{SI}{S+I}+\nu_1(x,t)E \\ -[\mu(x,t)+\omega(x,t)+\alpha(x,t)]L \end{array}, \; L \right\rangle_{\mathbf{H}} \\ = & \int_\Omega \beta_1(x,t)\frac{SL^2}{S+L}dx+\int_\Omega \beta_2(x,t)\frac{SLI}{S+I}dx \\ & +\int_\Omega \nu_1(x,t)ELdx-\int_\Omega[\mu(x,t)+\alpha(x,t)+\delta(x,t)]L^2dx \\ \leq & \beta_1^*\int_\Omega L^2dx+\beta_2^*\int_\Omega LIdx+\nu_1^*\int_\Omega ELdx, \end{aligned}$$

$$\begin{aligned} & \left\langle \delta(x,t)\frac{ST}{S+T}+\omega(x,t)L-[\mu(x,t)+\gamma(x,t)+\sigma(x,t)]T,T \right\rangle_{\mathbf{H}} \\ = & \int_\Omega \delta(x,t)\frac{ST^2}{S+T}dx+\int_\Omega \omega(x,t)LTdx \\ & -\int_\Omega[\mu(x,t)+\gamma(x,t)+\sigma(x,t)]T^2dx \end{aligned}$$

$$
\begin{aligned}
&\leq \delta^* \int_\Omega T^2 dx + \omega^* \int_\Omega LT dx,\\
&\left\langle \begin{array}{c} \gamma(x,t)T + k\sigma(x,t)\frac{ST}{S+T} \\ -[\mu(x,t)+\eta_1(x,t)+\nu_1(x,t)+\nu_2(x,t)+\theta_1(x,t)]E \end{array}, E \right\rangle_{\mathbf{H}}\\
&= \int_\Omega \gamma(x,t)ETdx + \int_\Omega k\sigma(x,t)\frac{SET}{S+T}dx\\
&\quad - \int_\Omega [\mu(x,t)+\eta_1(x,t)+\nu_1(x,t)+\nu_2(x,t)+\theta_1(x,t)]E^2 dx\\
&\leq \gamma^* \int_\Omega ETdx + k\sigma^* \int_\Omega ETdx,
\end{aligned}
$$

$$
\begin{aligned}
&\left\langle \begin{array}{c} \alpha(x,t)L + \sigma(x,t)T + \nu_2(x,t)E + \rho(x,t)R \\ -[\mu(x,t)+\eta_2(x,t)+\phi(x,t)]I \end{array}, I \right\rangle_{\mathbf{H}}\\
&= \int_\Omega \alpha(x,t)LIdx + \int_\Omega \sigma(x,t)ITdx + \int_\Omega \nu_2(x,t)EIdx\\
&\quad + \int_\Omega \rho(x,t)IRdx - \int_\Omega [\mu(x,t)+\eta_2(x,t)+\phi(x,t)]I^2 dx\\
&\quad \leq \alpha^* \int_\Omega LIdx + \sigma^* \int_\Omega ITdx + \nu_2^* \int_\Omega EIdx + \rho^* \int_\Omega IRdx,
\end{aligned}
$$

$$
\begin{aligned}
&\langle \phi(x,t)I - [\mu(x,t)+\eta_3(x,t)+\rho(x,t)+\theta_2(x,t)]R, R\rangle_{\mathbf{H}}\\
&= \int_\Omega \phi(x,t)IRdx - \int_\Omega [\mu(x,t)+\eta_3(x,t)+\rho(x,t)+\theta_2(x,t)]R^2 dx\\
&\leq \phi^* \int_\Omega IRdx,
\end{aligned}
$$

$$
\begin{aligned}
&\langle \theta_1(x,t)E + \theta_2(x,t)R - \mu(x,t)H, H\rangle_{\mathbf{H}}\\
&= \int_\Omega \theta_1(x,t)EHdx + \int_\Omega \theta_2(x,t)RHdx - \int_\Omega \mu(x,t)H^2 dx\\
&\leq \theta_1^* \int_\Omega EHdx + \theta_2^* \int_\Omega RHdx.
\end{aligned}
$$

From Theorem 2, we know the solution of system (1)

$$u = (S(x,t), L(x,t), T(x,t), E(x,t), I(x,t), R(x,t), H(x,t))$$

is uniformly bounded, hence, from above the inner product estimation, we can obtain that there exists a constant $C > 0$, such that

$$\langle G(t,u), u\rangle_{\mathbf{H}^7} \leq C,$$

then condition (4) holds. On the other hand, as we know that

$$
\begin{aligned}
A \quad = \quad & (\nabla\cdot(d_S(x)\nabla), \nabla\cdot(d_L(x)\nabla), \nabla\cdot(d_T(x)\nabla), 0, \nabla\cdot(d_I(x)\nabla),\\
& \nabla\cdot(d_R(x)\nabla), \nabla\cdot(d_H(x)\nabla))
\end{aligned}
$$

is a symmetrical sectorial operator and all eigenvalues of L are

$$0 > \lambda_1 \geq \lambda_2 \geq \cdots \geq \lambda_K > \ldots, \ \lambda_K \to -\infty \ (K \to \infty),$$

therefore, by Theorem 1, we can obtain that system (1) has a global exponentially attracting set $\mathcal{A}^*$. □

After verifying the global exponentially attracting set, we can use our methods in [6,17] similarly to discuss the stability and uniform persistance of the COVID-19 epidemic,

which was intervened upon by an epidemiological investigation. It is clearly observed that system (1) demonstrates a disease-free equilibrium $E^0(x) = (S^0(x), 0, 0, 0, 0, 0, 0)$. Linearize the last six equations of the system (1) at the disease-free equilibrium and let $L = e^{\lambda t}\chi(x), T = e^{\lambda t}\varphi(x), E = e^{\lambda t}\psi(x), I = e^{\lambda t}\xi(x), R = e^{\lambda t}\zeta(x), H = e^{\lambda t}\varrho(x)$; we can obtain the following characteristic equation system (10) corresponding to the last six equations of system (1)

$$\begin{cases} \lambda\Phi(x) = \nabla \cdot (D(x)\nabla\Phi(x)) + M(x,t)\Phi(x), \ x \in \Omega, \\ \frac{\partial\Phi}{\partial \mathbf{n}} = 0, \ x \in \partial\Omega, \end{cases} \tag{10}$$

where $\Phi(x) = (\chi(x), \varphi(x), \psi(x), \xi(x), \zeta(x), \varrho(x))^T$,

$$D(x) = \begin{bmatrix} d_L(x) & 0 & 0 & 0 & 0 & 0 \\ 0 & d_T(x) & 0 & 0 & 0 & 0 \\ 0 & 0 & 0 & 0 & 0 & 0 \\ 0 & 0 & 0 & d_I(x) & 0 & 0 \\ 0 & 0 & 0 & 0 & d_R(x) & 0 \\ 0 & 0 & 0 & 0 & 0 & d_H(x) \end{bmatrix}$$

and

$$\begin{aligned} & M(x,t) \\ = \ & (m_{ij}(x,t)) \\ = \ & \begin{bmatrix} m_{11}(x,t) & 0 & \nu_1(x,t) & \beta_2(x,t) & 0 & 0 \\ \omega(x,t) & m_{22}(x,t) & 0 & 0 & 0 & 0 \\ 0 & \gamma(x,t) + k\sigma(x,t) & m_{33}(x,t) & 0 & 0 & 0 \\ \alpha(x,t) & \sigma(x,t) & \nu_2(x,t) & m_{44}(x,t) & \rho(x,t) & 0 \\ 0 & 0 & 0 & \phi(x,t) & m_{55}(x,t) & 0 \\ 0 & 0 & \theta_1(x,t) & 0 & \theta_2(x,t) & -\mu(x,t) \end{bmatrix}, \end{aligned}$$

where

$$\begin{aligned} m_{11}(x,t) &= \beta_1(x,t) - [\mu(x,t) + \omega(x,t) + \alpha(x,t)], \\ m_{22}(x,t) &= \delta(x,t) - [\mu(x,t) + \gamma(x,t) + \sigma(x,t)], \\ m_{33}(x,t) &= -[\mu(x,t) + \eta_1(x,t) + \nu_1(x,t) + \nu_2(x,t) + \theta_1(x,t)], \\ m_{44}(x,t) &= -[\mu(x,t) + \eta_2(x,t) + \phi(x,t)], \\ m_{55}(x,t) &= -[\mu(x,t) + \eta_3(x,t) + \rho(x,t) + \theta_2(x,t)] \end{aligned}$$

and $m_{ij}(x) \geq 0, i \neq j, x \in \overline{\Omega}$. By the Krein–Rutman theorem, we can obtain that there exists a real principal eigenvalue λ^* of Equation (1) and a corresponding eigenvector $\Phi^*(x) >> 0$ for all $x \in \overline{\Omega}$ in the case of Neumann boundary conditions. Next, we use this principal eigenvalue as a threshold to characterize the spread trend of COVID-19.

Theorem 4. *The following statements are valid.*

(1) If $\lambda^* < 0$, then

$$\begin{aligned} \lim_{t\to\infty} S(x,t) &= S^0(x), \lim_{t\to\infty} L(x,t) = 0, \lim_{t\to\infty} T(x,t) = 0, \\ \lim_{t\to\infty} E(x,t) &= 0, \lim_{t\to\infty} I(x,t) = 0, \lim_{t\to\infty} R(x,t) = 0, \lim_{t\to\infty} H(x,t) = 0 \end{aligned}$$

in **H**, *and hence, the disease-free equilibrium is globally asymptotically stable. In a biological sense, the COVID-19 epidemic can be effectively controlled and will eventually die out.*

(2) If $\lambda^* > 0$, then there exists a endemic equilibrium $(S^*(x), L^*(x), T^*(x), E^*(x), I^*(x), R^*(x), H^*(x))$, such that any solution (S, L, T, E, I, R, H) satisfies

$$\lim_{t\to\infty} S(x,t) = S^*(x), \lim_{t\to\infty} L(x,t) = L^*(x), \lim_{t\to\infty} T(x,t) = T^*(x),$$

$$\begin{aligned}\lim_{t\to\infty} E(x,t) &= E^*(x), \lim_{t\to\infty} I(x,t) = I^*(x), \lim_{t\to\infty} R(x,t) = R^*(x),\\ \lim_{t\to\infty} H(x,t) &= H^*(x)\end{aligned}$$

for $x \in \overline{\Omega}$, and hence, the endemic equilibrium is globally asymptotically stable. In a biological sense, the COVID-19 epidemic continues to coexist with human beings.

Proof.

(1) The proof can be obtained by a similar method in the literature [6,17,22].

(2) Similar to the proof in [6,17], we can obtain that there exists a function $m(x) > 0$ independent of the initial data, such that any solution (S, L, T, E, I, R) satisfies

$$\begin{aligned}\liminf_{t\to\infty} S(x,t) &\geq m(x), \liminf_{t\to\infty} L(x,t) \geq m(x),\\ \liminf_{t\to\infty} T(x,t) &\geq m(x), \liminf_{t\to\infty} E(x,t) \geq m(x),\\ \liminf_{t\to\infty} I(x,t) &\geq m(x), \liminf_{t\to\infty} R(x,t) \geq m(x),\\ \liminf_{t\to\infty} H(x,t) &\geq m(x)\end{aligned} \tag{11}$$

for $x \in \overline{\Omega}$, and hence, the disease persists uniformly. According to the proof of the global exponentially attracting set in [19], it can be observed that global exponentially attracting set $\mathcal{A}^*$ contains the global attractor $\mathcal{A}$. By Theorem A.2.2 of [23], we can obtain that there exists an equilibrium $(S^*(x), L^*(x), T^*(x), E^*(x), I^*(x), R^*(x), H^*(x))$, such that any solution (S, L, T, E, I, R, H) satisfies

$$\begin{aligned}\lim_{t\to\infty} S(x,t) &= S^*(x), \lim_{t\to\infty} L(x,t) = L^*(x),\\ \lim_{t\to\infty} T(x,t) &= T^*(x), \lim_{t\to\infty} E(x,t) = E^*(x),\\ \lim_{t\to\infty} I(x,t) &= I^*(x), \lim_{t\to\infty} R(x,t) = R^*(x),\\ \lim_{t\to\infty} H(x,t) &= H^*(x).\end{aligned} \tag{12}$$

It follows from (11) that the equilibrium is not the disease-free equilibrium and the each limit of (12) is not equal to 0; thus, this equilibrium is the endemic equilibrium. Hence, the endemic equilibrium is globally asymptotically stable. □

3. Effect Simulation of Epidemiological Investigation

Previously, we provided a strict mathematical proof for the long-term dynamic behavior of the model. Although the global attractor theory is a commonly used method in infinite dimensional dynamic systems, the validation conditions we provided in this article are different from the validation methods in other existing conclusions. The validation conditions we provide are more convenient and can be easily used by researchers even for those who are not majoring in mathematics, which is also an innovation of this article. In order to understanding our theoretical results more intuitively, we will simulate the impact of different epidemic investigation strategies on the epidemic. These epidemic investigation strategies really exist during different periods of China's fight against COVID-19. Since we want to simulate the long-term dynamic behavior of COVID-19, we innovatively used 0 as the initial value of the compartments in the program for drawing three-dimensional images and select the month as the unit for the time axis.

3.1. Stability and Persistence of COVID-19 in China under the Dynamic Clearing Policy

Before December 2022, the Chinese government has been strictly implementing the prevention and control policy of dynamic clearing and has achieved remarkable results. With the help of official authoritative data and reasonable estimates, we focus on modeling the impact of the interregional movement and epidemiological investigations on

the prevention and control of COVID-19. According to the policy of the epidemiological investigation, people who live with or have contact with confirmed or asymptomatic infected persons are the objects of the key investigation. Therefore, the proportional coefficient of the epidemiological investigation of returnees from travel should be greater than 1. In addition, compartment H has little effect on the entire disease spreading process; we focus on simulating the changes of the first six compartments. The specific data are shown in Table 2. Part of the data in Table 2 comes from authoritative official data and part comes from reasonable estimates, which are not arbitrary. Our estimate is based on rigorous mathematical calculations [8,24] using actual official published data within a reasonable range.

Table 2. The parameters' description of the COVID-19 epidemic in China.

Parameter	Data Estimated	Data Sources
Λ	8	Calculate
β_1	0.6	Reference [6]
β_2	0.3	Reference [6]
α	0.6	Reference [25]
ω	0.1	Reference [25]
γ	0.7	Reference [25]
ν_1	0.0003	Calculate
ν_2	0.0002	Calculate
θ_1	0.7	Calculate
θ_2	0.8	Calculate
ρ	0.002	Reference [6]
ϕ	0.8	Reference [25]
μ	0.1595	Reference [26]
η_1	0.021	Reference [25]
η_2	0.047	Reference [25]
η_3	0.021	Reference [25]
δ	0.2	Calculate
σ	0.2	Calculate
k	1.7	Calculate
d_S	3	Calculate
d_L	2.5	Calculate
d_T	5	Calculate
d_I	0.3	Reference [22]
d_R	2	Reference [22]

Refering to the data in Table 2 and our system (1), we first simulate the spread trend of the novel coronavirus pneumonia epidemic in China (Figure 2).

The image is a more realistic projection of the current spread of the COVID-19 epidemic in China. From the graph, we can observe that COVID-19 is persistent.

If we choose $\beta_1 = 0.006$, $\beta_2 = 0.003$ in Table 2, then we can obtain the image in Figure 3. At this time, the disease-free equilibrium is globally asymptotically stable.

3.2. Comparison of Prevention and Control under Different Proportions of Epidemiological Investigation

Our model focuses on an epidemiological investigation and the impact of interregional movement on the prevention and control of COVID-19. Through research, we found that the degree of control of an epidemiological investigation has an impact on people's desire to travel. Close range activities related to life will continue but also decrease accordingly. When the epidemic investigation policy is tightened, people will go out as little as possible. In order to clearly observe the impact of the epidemiological investigation, we design three epidemiological investigation strategies with different levels. By comparison, we can find

that different epidemiological investigations have different effects on COVID-19 prevention and control. First, we focus on the epidemiological investigation of close and sub-close contacts of infected populations. The parameter k in the model represents the proportion of an epidemiological investigation of contact between the susceptible person and the infected person after interregional movement, which essentially describes the scope of the susceptible person, close contact and sub-close contact participating in the epidemiological investigation. We choose $k = 1.7$ and $k = 3$, respectively, to simulate the changes of T, E and I (Figure 4).

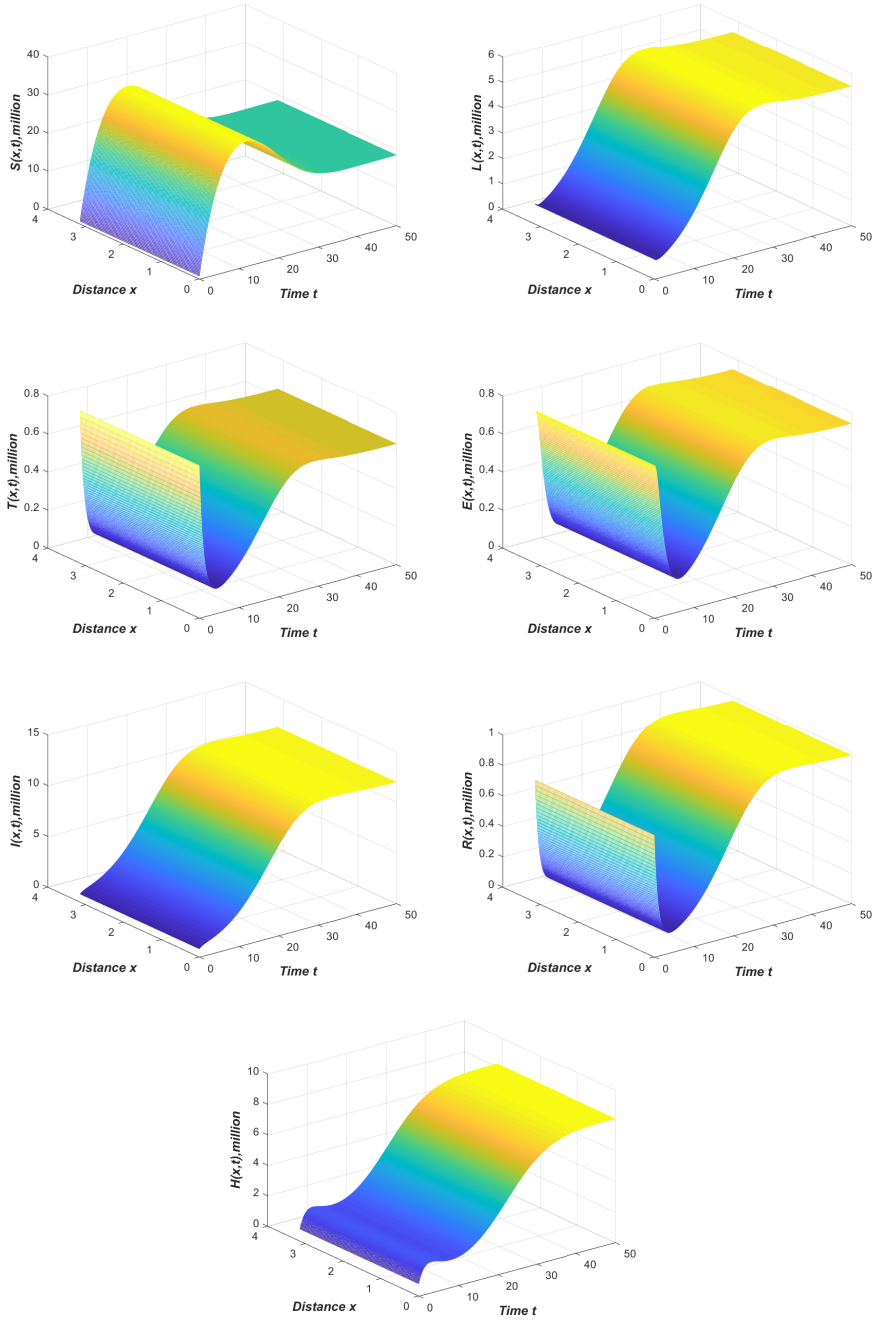

Figure 2. The spread trend of COVID-19 in China.

If the contact rate is very low (for example $\beta_1 = \beta_2 = 10^{-5}$), the probability of susceptible individuals being infected is very low, and the epidemic will disappear.

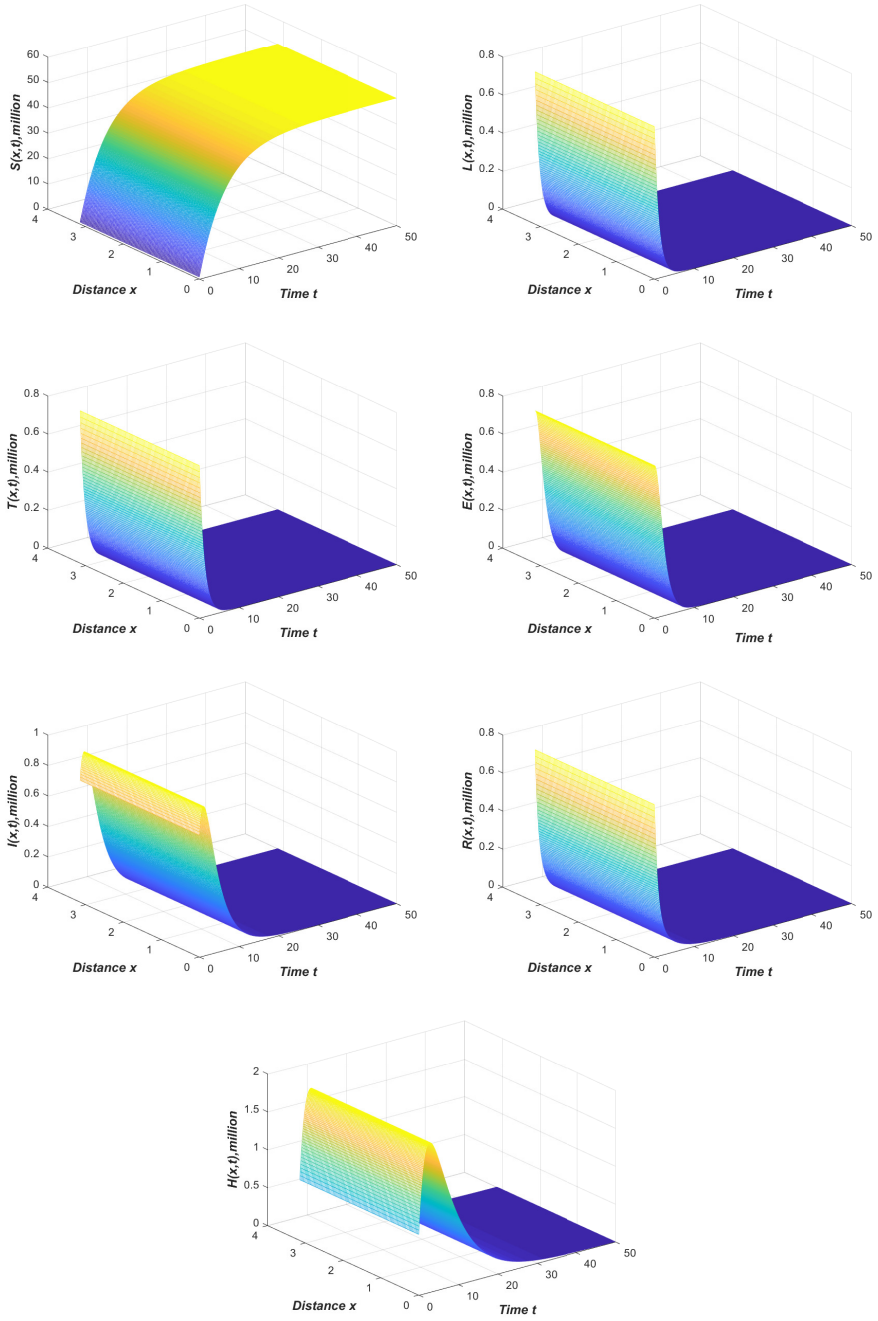

Figure 3. The global stability of disease-free equilibrium of constant coefficient COVID-19 model.

From the Figure 4, we can clearly observe when the scope of the epidemiological investigation expands ($k = 3$), the number of people participating in the epidemiological investigation increases, and strict policies lead to a significant decrease in people transferring between regions. Due to the increase in the proportion of the epidemiological investigation of co-living people, everyone clearly understands that the risk factor of the current epidemic is at a high level; thus, people's desire to go out has decreased significantly. At this stage, everyone can avoid travel unless necessary. On the other hand, expanding testing will also find more infected people.

Next, we examine the epidemiological investigation rate of the population that has moved between regions. We choose $\gamma = 0.3$ and $\gamma = 0.7$, respectively, to simulate the changes of T, E and I (Figure 5).

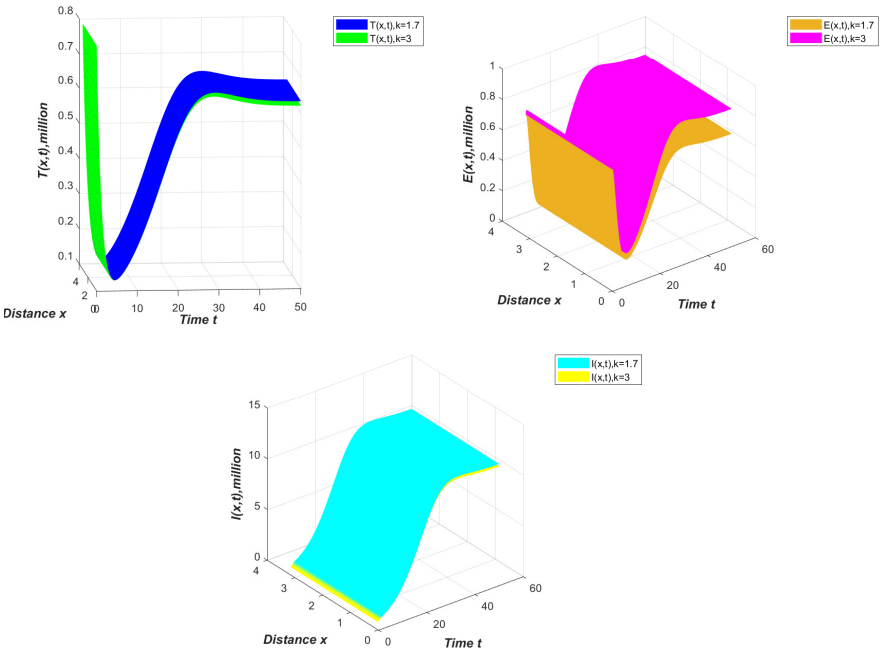

Figure 4. Comparison of compartment T, E and I under $k = 1.7$ and $k = 3$.

From Figure 5, we can find that implementing a strict epidemiological investigation policy can effectively reduce the number of movement between regions, the number of epidemiological investigations and the number of infected people. Strengthening the epidemiological investigation can effectively control the diffusion of COVID-19.

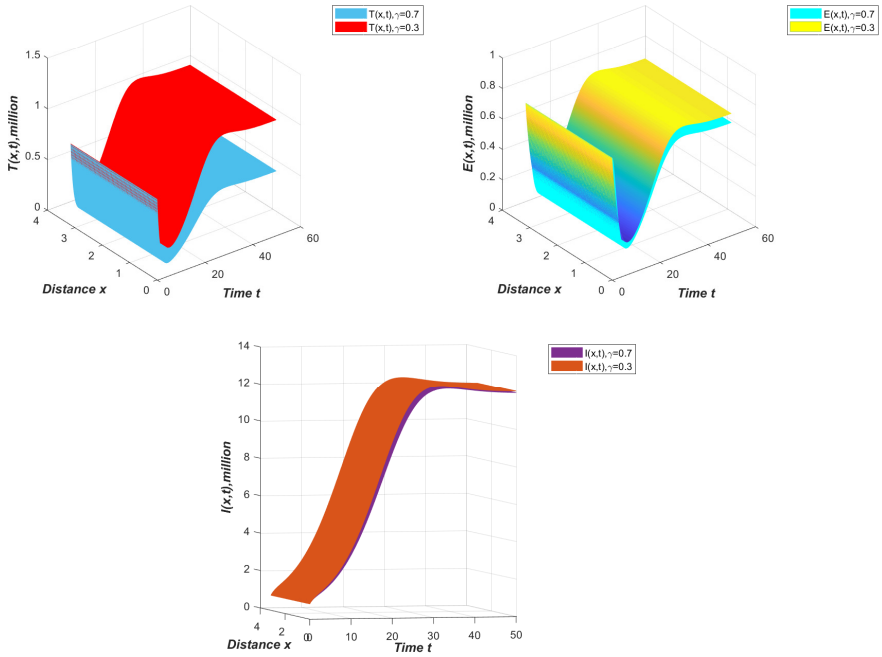

Figure 5. Comparison of compartment T, E and I under $\gamma = 0.3$ and $\gamma = 0.7$.

In Figure 6, while expanding the scope of the epidemiological investigation, we also increased the proportion of the epidemiological investigation. We find that the final effect of this prevention and control policy is similar to Figure 4, because the proportion of the epidemiological investigation of transferors is increased, and the time to find infected people is earlier than that of only expanding the detection scope of the co-living. The strict epidemiological investigation policy shown in Figure 5 has bought more time for the

prevention and control of the epidemic, so that infected persons and close contacts can be detected as early as possible, and the further spread of the epidemic can be controlled. The strict epidemiological investigation in Figure 6 is an important part of the current Chinese government's dynamic clearing policy.

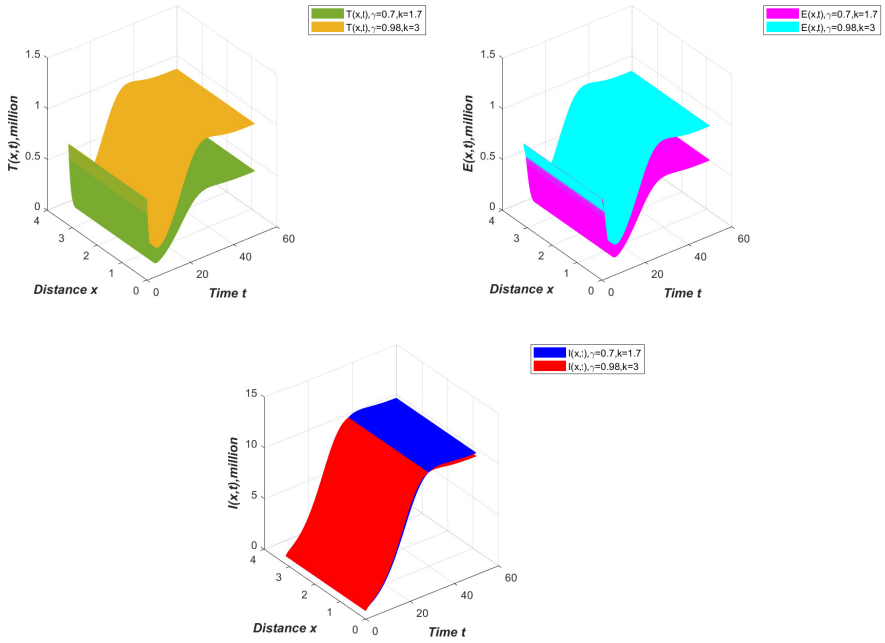

Figure 6. Comparison of compartment T, E and I under different rates of epidemiological investigation.

3.3. Effect of Prevention and Control under Circuit-Breaker Mechanism

In China, the dynamic clearing policy requires that once a confirmed case is found in a certain area, the government will quickly carry out a strict epidemiological investigation, including closure and control management, nucleic acid for all employees, and quarantine and treatment in designated hospitals. The Civil Aviation of China has also introduced stricter prevention and control measures for inbound flights. Once the number of positive passengers exceeds 5, the flight will be grounded. This extremely tight control is also known as a circuit-breaker mechanism. The circuit breaker mechanism is also reflected in our model. Lockdown management and travel restrictions will reduce the travel rate to zero, that is, the parameter $\delta = \omega = 0$ in our model. The centralized quarantine can effectively reduce the contact rate, especially the contact rate with confirmed patients, that is, $\beta_2 = 0$. After considering a strong circuit-breaker mechanism, our model (1) can be evolved, as in Figure 7:

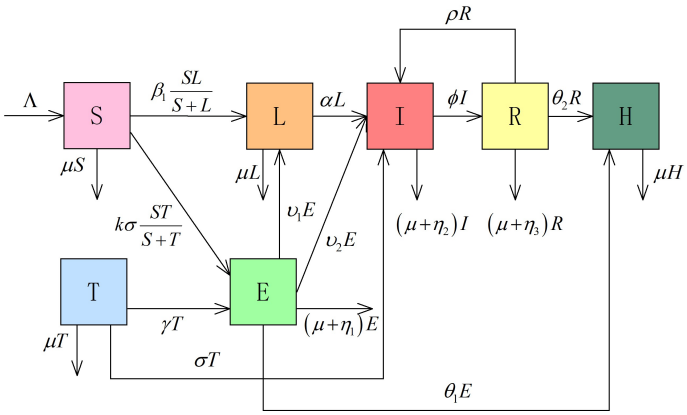

Figure 7. Dynamic clearing COVID-19 model with circuit-breaker mechanism.

The equations corresponding to the evolution model is shown in system (13),

$$\begin{cases} \frac{\partial S}{\partial t} = \nabla \cdot (d_S(x)\nabla S) + \Lambda(x,t) - \beta_1(x,t)\frac{SL}{S+L} - k\sigma(x,t)\frac{ST}{S+T} - \mu(x,t)S, \\ \frac{\partial L}{\partial t} = \nabla \cdot (d_L(x)\nabla L) + \beta_1(x,t)\frac{SL}{S+L} + \nu_1(x,t)E - [\mu(x,t) + \alpha(x,t)]L, \\ \frac{\partial T}{\partial t} = \nabla \cdot (d_T(x)\nabla T) - [\mu(x,t) + \gamma(x,t) + \sigma(x,t)]T, \\ \frac{\partial E}{\partial t} = \gamma(x,t)T + k\sigma(x,t)\frac{ST}{S+T} \\ \quad - [\mu(x,t) + \eta_1(x,t) + \nu_1(x,t) + \nu_2(x,t) + \theta_1(x,t)]E, \\ \frac{\partial I}{\partial t} = \nabla \cdot (d_I(x)\nabla I) + \alpha(x,t)L + \sigma(x,t)T + \nu_2(x,t)E + \rho(x,t)R \\ \quad - [\mu(x,t) + \eta_2(x,t) + \phi(x,t)]I, \\ \frac{\partial R}{\partial t} = \nabla \cdot (d_R(x)\nabla R) + \phi(x,t)I - [\mu(x,t) + \eta_3(x,t) + \rho(x,t) + \theta_2(x,t)]R, \\ \frac{\partial H}{\partial t} = \nabla \cdot (d_H(x)\nabla H) + \theta_1(x,t)E + \theta_2(x,t)R - \mu(x,t)H, \\ \quad x \in \Omega, t > 0, \\ \frac{\partial S}{\partial \mathbf{n}} = \frac{\partial L}{\partial \mathbf{n}} = \frac{\partial T}{\partial \mathbf{n}} = \frac{\partial E}{\partial \mathbf{n}} = \frac{\partial I}{\partial \mathbf{n}} = \frac{\partial R}{\partial \mathbf{n}} = \frac{\partial H}{\partial \mathbf{n}} = 0, \ x \in \partial\Omega, t > 0, \\ S(x,s) = S_0(x,s) \geq 0, L(x,s) = L_0(x,s) \geq 0, T(x,s) = T_0(x,s) \geq 0, \\ E(x,s) = E_0(x,s) \geq 0, I(x,s) = I_0(x,s) \geq 0, R(x,s) = R_0(x,s) \geq 0, \\ H(x,s) = H_0(x,s) \geq 0, x \in \Omega, -\tau \leq s \leq 0. \end{cases} \tag{13}$$

The global dynamic behavior of the model (13) can also be obtained by the method in the previous section.

Combined with the actual COVID-19 epidemic prevention and control, we can find that under the powerful circuit-breaker mechanism, asymptomatic infections and confirmed patients will be quarantined in a centralized manner, and they have no possibility of diffusion at all. Other groups of people in the area will also be in a state of restricted movement due to the sealing policy. They can only move within the community, and the living materials are uniformly distributed by the government. Therefore, the diffusion coefficients in model (13) are all equal to 0 or tend to 0 under the circuit-breaker mechanism. Next, we simulate the model with the circuit-breaker mechanism. Select $\delta = \omega = \beta_2 = 0$, and other data will still use the data in Table 2; then, we obtain Figure 8.

From Figure 8, we can clearly observe that after cutting off contact and travel for the first time, with high-density nucleic acid detection, the effect of epidemic control has been greatly improved. At this time, the model tends to have a disease-free equilibrium and is globally asymptotically stable. Comparing Figure 2, we can find that the other simulated data are identical except for $\delta = \omega = \beta_2 = 0$. However, Figure 2 tends towards the endemic equilibrium. This demonstrates that the circuit-breaker mechanism can control the diffusion of COVID-19 faster and make the disease disappear.

3.4. Epidemic Situation in China after the Opening of Epidemiological Investigation Policy

On 7 December 2022, the Chinese government released the policy of epidemic prevention and control. Epidemiological investigations such as trip codes and all staff nucleic acids were cancelled. In the following month, as many as 70% of Chinese people were infected with COVID-19, and the convalescents began to travel in large numbers. According to the data officially released by China, from 8 December 2022 to 12 December 2023, there were 59,938 deaths related to COVID-19 in hospitals in medical institutions across the country, including 54,435 deaths from underlying diseases combined with COVID-19 infection. The average age of death cases is 80.3 years, and more than 90% of them are accompanied by basic diseases.

If we choose $k = \gamma = \nu_1 = \nu_2 = \theta_1 = \eta_1 = 0$ in system (1), we can simulate the current COVID-19 diffusion trend in China and the state of the people.

By comparing Figure 2 and Figure 9, we can find that the number of people moving between regions has increased significantly since the epidemiological survey was released. Due to the lack of mandatory nucleic acid testing, the number of asymptomatic patients and infected persons has also increased significantly. Because multiple strains of viruses

coexist in China, the number of secondary infections and relapses has also increased dramatically, and the number of completely cured patients has decreased. This comparison just demonstrates that the epidemiological investigation has a very good control over the spread of global infectious diseases. Although COVID-19 is now classified as a Class B infectious disease, an epidemiological investigation is still an effective means to control the epidemic situation when the number of infected people increases sharply due to the virus mutation. Epidemiological investigation can also be used for reference when dealing with other global epidemics in the future.

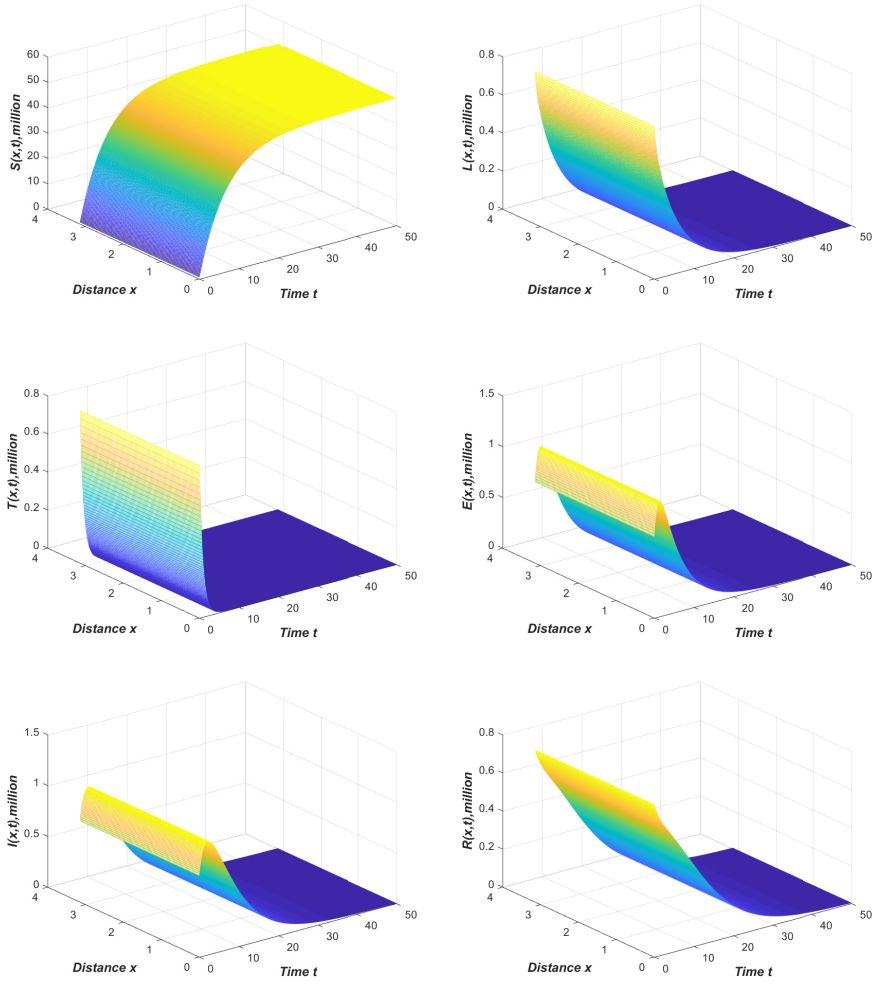

Figure 8. The dynamics of temporal-spatial heterogeneity in COVID-19 epidemic with circuit-breaker mechanism when $\delta = \omega = \beta_2 = 0$.

Based on the previous introduction, we know that in December 2022, the Chinese government cancelled the strategy of conducting epidemic investigations and instead monitored key populations. There has been a surge in social infections. We have compiled the cumulative confirmed cases announced on the official website of the Chinese Health Commission in December (starting on 24 December 2022, the Chinese government no longer released data on a daily basis).

We have listed the data for December 2022 in Table 3.

Comparing the above data with the number of infected individuals simulated by our model, we can draw the following simulation diagram, in which we select the initial value of 30,000 people in the infected person's compartment.

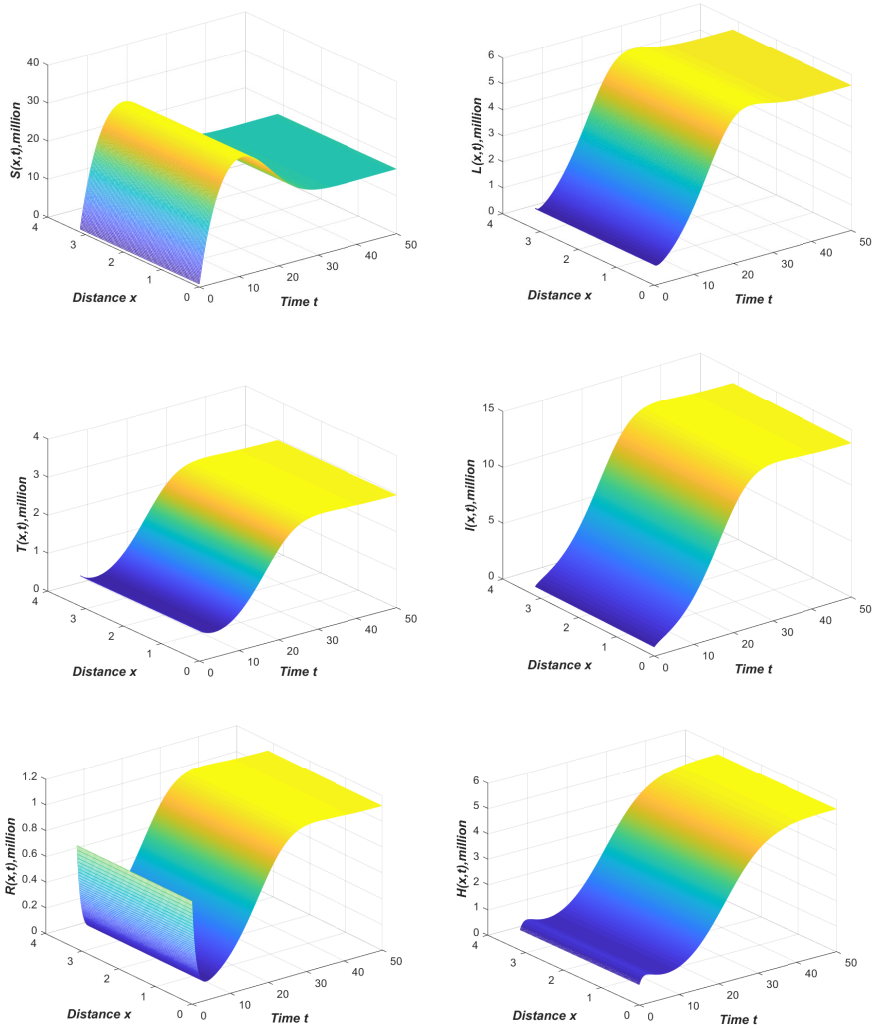

Figure 9. The spread trend of the COVID-19 in China without epidemiological investigation.

Table 3. Total confirmed cases in China from December 1st to December 23rd.

Date	Total Confirmed Cases	Date	Total Confirmed Cases
1 Dec. 2022	327,964	2 Dec. 2022	331,952
3 Dec. 2022	336,165	4 Dec. 2022	340,483
5 Dec. 2022	345,529	6 Dec. 2022	349,938
7 Dec. 2022	354,017	8 Dec. 2022	357,652
9 Dec. 2022	360,734	10 Dec. 2022	363,072
11 Dec. 2022	365,312	12 Dec. 2022	367,627
13 Dec. 2022	369,918	14 Dec. 2022	371,918
15 Dec. 2022	374,075	16 Dec. 2022	376,361
17 Dec. 2022	378,458	18 Dec. 2022	380,453
19 Dec. 2022	383,175	20 Dec. 2022	386,276
21 Dec. 2022	389,306	22 Dec. 2022	393,067
23 Dec. 2022	397,195	24 Dec. 2022	None

From Figure 10, we can observe that the simulation effect of our model is in good agreement with the actual data.

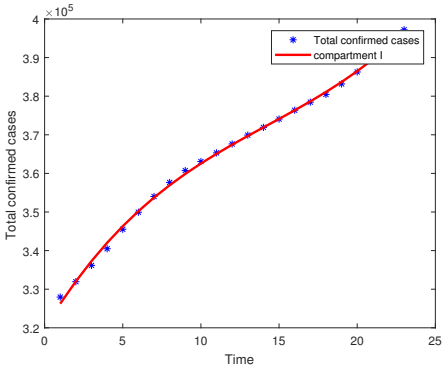

Figure 10. Comparison between official data and compartment simulation.

In the numerical simulation above, we simulated the prevention and control effects of various epidemiological investigations. We summarize the four most important categories as follows:

1. If the data in Table 2 is selected, the endemic equilibrium is globally asymptotically stable.
2. If the contact rate is very low, the disease-free equilibrium is globally asymptotic and stable.
3. If it is a circuit-breaker mechanism, the disease-free equilibrium is globally asymptotic and stable.
4. When opening the epidemiological investigation policy; the endemic equilibrium is globally asymptotically stable.

4. Conclusions

By 2023, the global COVID-19 epidemic has been effectively controlled, but there are still sporadic outbreaks in some countries. In April 2023, India experienced another wave of COVID-19 outbreaks. Experts also predict that China will have a second wave of COVID-19 from May to June 2023. Therefore, daily monitoring and prevention cannot be relaxed. In this paper, we focused on the impact of epidemiological investigation policies on the COVID-19 outbreak. In order to more intuitively demonstrate the practicality of our results, we discuss the impact of the epidemiological investigation on epidemic prevention and control in light of the current spread of the COVID-19 epidemic. Using Theorem 1, we can obtain that system (1) has a global exponentially attracting set $\mathcal{A}^*$, then we prove that the COVID-19 model with travel and an epidemiological investigation persists uniformly and that the model has a global exponentially attracting set. Compared with the results in [17], the condition (4) in this article is easier to verify, and the amount of calculation is much less. Our model covers epidemiological investigations at different stages of the COVID-19 epidemic in China. By selecting appropriate parameters to simulate, we provide intuitive results of various epidemiological investigation policies. Although the current COVID-19 epidemic has achieved good control results, other diseases such as the influenza A virus still pose a threat to human health, and the coronavirus may undergo further mutations in the future. The epidemiological investigation experience accumulated during the COVID-19 epidemic can be applied to the prevention and control of other diseases.

The COVID-19 epidemic in China has been effectively controlled, with occasional recurrences and new cases emerging. Based on the current situation of epidemic prevention and control, it is recommended that the Chinese government strengthen the popularization of public health knowledge. Conduct necessary epidemiological investigations on key populations, such as those entering the epidemic area, newly diagnosed and relapsed individuals and their close contacts, and effectively monitor the variation of domestic strains.

Through research, we find that the global exponential attractor theory is more convenient than the Lyapunov method in discussing the long-term dynamic behavior of multi equation coupled systems, and the verification conditions provided in this paper are conve-

nient for researchers of different research directions. Although the COVID-19 pandemic has become a thing of the past in most countries, epidemiological investigations as a prevention and control strategy can be borrowed from the prevention and control of other diseases.

Author Contributions: Methodology, C.-C.Z., J.Z. and J.S.; Formal analysis, J.Z.; Writing—original draft, C.-C.Z. and J.Z.; Writing—review & editing, C.-C.Z., J.Z. and J.S. All authors have read and agreed to the published version of the manuscript.

Funding: This work was supported by the Natural Science Foundation of Jiangsu Province, China (Grant No. BK20190578).

Data Availability Statement: The data in this article are all public data published on the official websites of the World Health Organization, the Chinese Health Commission and everyone can check them on the corresponding websites.

Conflicts of Interest: The authors declare that they have no competing interests.

References

1. Feng, L.X.; Jing, S.L.; Hu, S.K.; Wang, D.F.; Huo, H.F. Modelling the effects of media coverage and quarantine on the COVID-19 infections in the UK. *Math. Biosci. Eng.* **2020**, *17*, 3618–3636. [CrossRef]
2. Feng, X.; Chen, J.; Wang, K.; Wang, L.; Zhang, F.; Jin, Z.; Zou, L.; Wang, X. Phase-adjusted estimation of the COVID-19 outbreak in South Korea under multi-source data and adjustment measures: A modelling study. *Math. Biosci. Eng.* **2020**, *17*, 3637–3648. [CrossRef]
3. Machado, B.; Antunes, L.; Caetano, C.; Pereira, J.F.; Nunes, B.; Patricio, P.; Morgado, M.L. The impact of vaccination on the evolution of COVID-19 in Portugal. *Math. Biosci. Eng.* **2021**, *19*, 936–952. [CrossRef] [PubMed]
4. Suzuki, A.; Nishiura, H. Transmission dynamics of varicella before, during and after them COVID-19 pandemic in Japan: A modelling study. *Math. Biosci. Eng.* **2022**, *19*, 5998–6012. [CrossRef] [PubMed]
5. Yang, C.; Wang, J. Modeling the transmission of COVID-19 in the USA case study. *Infect. Dis. Model.* **2021**, *6*, 195–211.
6. Zhu, C.C.; Zhu, J. The effect of self-limiting on the prevention and control of the diffuse COVID-19 epidemic with delayed and temporal-spatial heterogeneous. *BMC Infect. Dis.* **2021**, *21*, 1145. [CrossRef]
7. Dai, Y.; Zhang, R.; Jiang, Y.; Jin, H.; Zhao, J.; Guo, A.; Chen, X.; Fan, D.; Yang, L. Infection control management strategy for operating room during COVID-19 pandemic. *Ann. Transl. Med.* **2022**, *10*, 1252. [CrossRef]
8. Luo, X.F.; Feng, S.; Yang, J.; Peng, X.L.; Cao, X.; Zhang, J.; Yao, M.; Zhu, H.; Li, M.Y.; Wang, H.; et al. Nonpharmaceutical interventions contribute to the control of COVID-19 in China based on a pairwise model. *Infect. Dis. Model.* **2021**, *6*, 643–663. [CrossRef]
9. Mbogo, R.W.; Orwa, T.O. SARS-COV-2 outbreak and control in Kenya-Mathematical model analysis. *Infect. Dis. Model.* **2021**, *6*, 370–380 [CrossRef] [PubMed]
10. Sabirli, R.; Koseler, A.; Goren, T. High GRP78 levels in Covid-19 infection: A case-control study. *Life Sci.* **2021**, *265*, 118781. [CrossRef]
11. Tang, K.H.D.; Chin, B.L.F. Correlations between control of COVID-19 transmission and influenza occurrences in Malaysia. *Public Health* **2021**, *198*, 96–101. [CrossRef]
12. Thongtha, A.; Modnak, C. Optimal COVID-19 epidemic strategy with vaccination control and infection prevention measures in Thailand. *Infect. Dis. Model.* **2022**, *7*, 835–855. [CrossRef]
13. Akter, S.; Jin, Z. A fractional order model of the COVID-19 outbreak in Bangladesh. *Math. Biosci. Eng.* **2022**, *20*, 2544–2565. [CrossRef] [PubMed]
14. Martinez-Fernandez, P.; Fernandez-Muniz, Z.; Cernea, A.; Fernandez-Martinez, J.L.; Kloczkowski, A. Three Mathematical Models for COVID-19 Prediction. *Mathematic* **2020**, *17*, 506. [CrossRef]
15. Childs, M.R.; Wong, T.E. Assessing parameter sensitivity in a university campus COVID-19 model with vaccinations. *Infect. Dis. Model.* **2023**, *8*, 374–389. [CrossRef]
16. Yang, H.; Lin, X.; Li, J. A Review of Mathematical Models of COVID-19 Transmission. *Contemp. Math.* **2023**, *4*, 75–98. [CrossRef]
17. Zhu, C.C.; Zhu, J. Spread trend of COVID-19 epidemic outbreak in China: Using exponential attractor method in a spatial heterogeneous SEIQR model. *Math. Biosci. Eng.* **2020**, *17*, 3062–3087. [CrossRef] [PubMed]
18. Zhu, C.C.; Zhu, J.; Liu, X.L. Influence of spatial heterogeneous environment on long-term dynamics of a reaction-diffusion SVIR epidemic model with relapse. *Math. Biosci. Eng.* **2019**, *16*, 5897–5922. [CrossRef]
19. Zhang, J.; Kloeden, P.E.; Yang, M.; Zhong, C.K. Global exponential κ-dissipative semigroups and exponential attraction. *Discrete Contin. Dyn. Syst.* **2017**, *37*, 3487–3502. [CrossRef]
20. Vrabie, I.I. C_0 *Semigroups and Application*; Elsevier Science BV: New York, NY, USA, 2003.
21. Wu, J. *Theory and Applications of Partial Functional Differential Equations*; Applied Mathematical Sciences; Springer: New York, NY, USA, 1996.

22. Zhu, C.C.; Zhu, J. Dynamic analysis of a delayed COVID-19 epidemic with home quarantine in temporal-spatial heterogeneous via global exponential attractor method. *Chaos Solitons Fractals* **2021**, *143*, 110546. [CrossRef]
23. Ma, T.; Wang, S. *Phase Transition Dynamics*; Springer Science+Business Media, LLC.: Berlin, Germany, 2014.
24. Tang, B.; Xia, F.; Bragazzi, N.L.; McCarthy, Z.; Wang, X.; He, S.; Sun, X.; Tang, S.; Xiao, Y.; Wu, J. Lessons drawn from China and South Korea for managing COVID-19 epidemic: Insights from a comparative modeling study. *ISA Trans.* **2022**, *124*, 164–175. [CrossRef] [PubMed]
25. Notification of Pneumonia Outbreak of New Coronavirus Infection. Available online: http://www.nhc.gov.cn; http://en.nhc.gov.cn (accessed on 1 January 2023).
26. World Health Statistics. 2013. Available online: http://www.who.int (accessed on 1 January 2023).